Neutralization of viral infectivity by zebrafish c-reactive protein isoforms

Melissa Bello-Perez[b], Alberto Falco[b], Regla Medina-Gali[b], Patricia Pereiro[c],
Jose Antonio Encinar[b], Beatriz Novoa[c], Luis Perez[b], Julio Coll[a],*

[a] Instituto Nacional Investigaciones y Tecnologías Agrarias y Alimentarias, Dpto. Biotecnología. INIA. Madrid, Spain
[b] Instituto de Biología Molecular y Celular, Universidad Miguel Hernández (IBMC-UMH). Elche, Spain
[c] Investigaciones Marinas.CSIC. Vigo, Spain

ARTICLE INFO

ABSTRACT

This work explores the unexpected in vivo and in vitro anti-viral functions of the seven c-reactive protein (crp1-7) genes of zebrafish (Danio rerio). First results showed heterogeneous crp1-7 transcript levels in healthy wild-type zebrafish tissues and organs and how those levels heterogeneously changed not only after bacterial but also after viral infections, including those in adaptive immunity-deficient rag1$^{-/-}$ mutants. As shown by microarray hybridization and proteomic techniques, crp2/CRP2 and crp5/CRP5 transcripts/proteins were among the most modulated during in vivo viral infection situations including the highest responses in the absence of adaptive immunity. In contrast crp1/CRP1/and crp7/CRP7 very often remained unmodulated. All evidences suggested that zebrafish crp2-6/CRP2-6 may have in vivo anti-viral activities in addition to their well known anti-bacterial and/or physiological functions in mammalians. Confirming those expectations, in vitro neutralization and in vivo protection against spring viremia carp virus (SVCV) infections were demonstrated by crp2-6/CRP2-6 using crp1-7 transfected and/or CRP1-7-enriched supernatant-treated fish cells and crp2-5-injected one-cell stage embryo eggs, respectively. All these findings discovered a crp1-7/CRP1-7 primitive anti-viral functional diversity.These findings may help to study similar functions on the one-gene-coded human CRP, which is widely used as a clinical biomarker for bacterial infections, tissue inflammation and coronary heart diseases.

1. Introduction

Widely used as a general biomarker for bacterial infection and inflammation during many decades, circulating human pentameric CRP (pCRP) has been found recently within atherosclerotic lesions and might be used as a new biomarker for cardiovascular diseases (Shrivastava et al., 2015). Correlation between infections and cardiovascular heart diseases has been demonstrated not only for bacteria but also for several viral infections (Adinolfi et al., 2014; McKibben et al., 2016; Voulgaris and Sevastianos, 2016; Wu et al., 2016). Furthermore, although pCRP was initially discovered during acute-phase responses to bacterial infections increasing their circulating levels from < 10 to > 500 mg/l, intermediate concentrations of 10–50 mg/l were also detected during viral infections (Shah et al., 2015), suggesting that pCRP may have also anti-viral function(s). At this respect, viral infections induce human interferon alpha that represses the crp promoter, suggesting also pCRP antiviral effects (Enocsson et al., 2009). Nevertheless and despite pCRP being one of the most investigated risk biomarker molecule in the human cardiovascular field, and an important component of the anti-bacterial innate responses (Vilahur and Badimon, 2015), to our knowledge, there is no evidence yet that pCRP has any antiviral function.

In contrast to the one-gene crp of humans, zebrafish (Danio rerio) has 7 crp genes, from crp1 to crp7 (here simplified as crp1-7 or CRP1-7 for their derived proteins). Amino acid variations among CRP1-7 proteins were mostly found in both their Ca^{++}-dependent phospholipid-binding pocket and conformational-domain sequences (Bello et al., 2017; Chen et al., 2015; Falco et al., 2012). By offering an easy-to-screen in vivo system for novel therapeutic molecules, zebrafish supplies a suitable model to explore CRP lipid-binding properties and conformation-dependent functionalities related to cardiovascular heart diseases including viral infections. Zebrafish is a well known model for heart development and function (Genge et al., 2016; Lu et al., 2016; Pitto et al., 2011) and a well known target for several fish rhabdoviruses (Encinas et al., 2013; Estepa and Coll, 2015a; Garcia-Valtanen et al., 2017; Varela et al., 2016). In this context, we have first explored crp1-7/CRP1-7 transcript/protein levels during several zebrafish viral infection situations and then designed several in vitro/in vivo strategies to explore

crp1-7/CRP1-7 implication on viral infections.

Zebrafish CRP1-7 are made of protein monomers of ∼ 200 amino acids (∼ 23 kDa)(Chen et al., 2015; Falco et al., 2012). According to its proposed 3D structure, CRP5 is a trimeric Ca^{++}-dependent phospholipid-binding protein (tCRP) rather than a pentameric molecule (pCRP) as in humans (Chen et al., 2015). It is not yet known whether all the rest of zebrafish CRP isoforms are also trimeric (Bello et al., 2017) and/or whether they all have similar functionalities than human pCRP. For instance, although C1q (a known ligand of pCRP) have been identified in zebrafish (Boshra et al., 2006), fish have only IgM and one class of polymeric immunoglobulin receptor (PIGR)(Zhang et al., 2010) (other IgG receptors bind C1q-pCRP complexes). There have been no reports on interactions between CRP1-7 and zebrafish C1q or PIGR (Lu et al., 2012). Therefore, the possible human analogous functions of the CRP1-7 isoforms remain unknown.

Human and zebrafish CRPs showed a high degree of conservation, including the location of their two cysteine residues, and similarities between the amino acid sequences involved in their Ca^{++}-dependent ligand-binding pockets. Such conservation suggested similar functions in human pCRP and zebrafish tCRPs (Bello et al., 2017; Chen et al., 2015). On the other hand, the variations of amino acids around the ligand-binding pockets of zebrafish CRPs, suggested different ligand-binding specificities, which may be hypothetically explained by the need to target a wide pathogen diversity such as that found in aquatic environments (Bello et al., 2017). Previous preliminary data showing modulation of zebrafish *crp*-pathways during viral infections (Estepa and Coll, 2015a; Garcia-Valtanen et al., 2017) or trout *crp* upregulation during oral vaccination against virus (Ballesteros et al., 2012), suggested that zebrafish *crp1-7*/CRP1-7 may have some anti-viral activities. Because all the above mentioned reasons, we have further studied possible relations between zebrafish individual *crp1-7*/CRP1-7 and viral infections.

As zebrafish viral infection models we mainly chose two rhabdoviruses to which zebrafish is susceptible, the Spring Viremia Carp Virus (SVCV) (Lopez-Munoz et al., 2010; Sanders et al., 2003), and the Viral Haemorrhagic Septicemia Virus (VHSV) (Novoa et al., 2006). Rhabdoviruses penetrate into the fish body via their fins (Harmache et al., 2006). The progress of infection becomes externally associated with exophthalmia, abdominal distension, and petechial haemorrhages in fins and gills 3 to 6 days after penetration. A few days later, the most important fish internal lymphoid organs such as head kidney and spleen become also affected (Ahne et al., 2002; Ashraf et al., 2016). Mortalities are highest ∼ 15 days after the beginning of infection (Encinas et al., 2013; Encinas et al., 2010).

To detect possible variations on *crp1-7*/CRP1-7 expression, we have explored several zebrafish infection situations. Thus, among the viral infection situations chosen, short-term (infection) and long-term responses (survival) were studied after infection with VHSV (Encinas et al., 2010; Estepa and Coll, 2015b) and SVCV (Encinas et al., 2013). Bacterial infections were also studied because of the well known antibacterial pCRP responses on humans (Kindmark, 1971). Since resistance to viral infections in both fish and mammalians depends both on innate and adaptive responses (i.e., neutralizing IgM antibodies in fish and both IgM/IgG antibodies in mammalians), fish rely more heavily in innate than in adaptive responses to fight viral infections (Sunyer, 2013; Sunyer et al., 1998). To explore the importance of *crp1-7* innate responses in the presence and absence of adaptive immunity, we studied adaptive immunity-deficient zebrafish *rag1*$^{-/-}$ mutants, which have no antibodies nor T-cell receptors and whose responses to viral infections have been studied recently (Garcia-Valtanen et al., 2017). Results showed heterogeneous *crp1-7* transcriptional profiles in all the above mentioned infection situations including higher responses in the absence of adaptive immunity, all results suggesting heterogeneous *crp1-7* anti-viral responses. Confirming those expectations, *in vitro* neutralization and *in vivo* protection of SVCV infection were found for the first time to be induced by the different zebrafish *crp1-7*/CRP1-7

isoforms. In addition to its possible implications to prevent and/or to treat human cardiovascular/viral diseases, this knowledge and future studies on their mechanism(s) of action may help to understand primitive vertebrate CRP diversity and how it may have evolved to humans. It also could be applied to improve prevention methods for viral infection in farmed fish.

2. Material and methods

2.1. Zebrafish (Danio rerio)

Adult XL wild type zebrafish of 700–900 mg of body weight (3–4 cm in length) were obtained from a local pet shop (Aquarium Madrid, Madrid, Spain). Zebrafish of 6 months of age (∼ 500 mg of body weight) with truncated-inactivated recombinant activation gene (*rag1*$^{-/-}$) and their corresponding wild-type *rag1*$^{+/+}$ counterparts were originally obtained from David Raible's fish facility at the University of Washington (USA) and raised, maintained, and characterized as described before (Garcia-Valtanen et al., 2017). Zebrafish were maintained at 24–28 °C in 30 l aquaria with tap-dechlorinated carbon-filtered water with 1 g of $CaCl_2$, 1 g of $NaHCO_3$ and 0.5 g of Instant Ocean sea salts added to water resulting in a conductivity of 200–300 μS and pH of 7.8-8.2. The aquaria were provided with biological filters and fish fed daily with a commercial feed diet (Vipan Bio-Vip, Sera, Heisenberg, Germany). Previously to the viral infection challenge, fish were acclimatized for 2 weeks to the corresponding optimal viral replication temperatures.

2.2. Fish cell culture

The *epithelioma papulosum cyprinid* (EPC) cells from the fathead minnow fish (*Pimephales promelas*) were obtained from the American Type Culture Collection (ATCC, Manassas, Vi, USA, code number CRL-2872). EPC cell monolayers were grown at 28 °C in a 5% CO_2 atmosphere in RPMI-1640 Dutch modified culture medium (Gibco, UK) supplemented with 20 mM HEPES, 10% fetal bovine serum, FBS (Sigma, St. Louis, USA), 1 mM piruvate, 2 mM glutamine, 50 μg/ml of gentamicin (Gibco) and 2 μg/ml of fungizone.

2.3. In vitro infections with viral haemorrhagic septicemia virus (VHSV) and spring viremia carp virus (SVCV)

The fish *novirhabdovirus* viral haemorrhagic septicemia virus (VHSV) strain 07.71 (accession number AJ233396) isolated from rainbow trout *Oncorhynchus mykiss* (LeBerre et al., 1977) and the rhabdovirus Spring Viremia Carp Virus (SVCV) isolate 56/70 from carp *Cyprinus carpio* (Fijan et al., 1971), recently renamed *Carp Sprivivirus* (ICTV, 2015), were used for *in vitro* and *in vivo* infections. VHSV or SVCV were replicated in EPC cell monolayers at 14 °C (Estepa and Coll, 2015a) or at 22 °C (Garcia-Valtanen et al., 2017), respectively, in the cell culture media described above except for 2% FBS (infection media) and absence of the CO_2 atmosphere. Supernatants from VHSV or SVCV-infected EPC cell monolayers were clarified by centrifugation at 4000 g for 30 min and kept at −80 °C. *In vitro* viral infections were performed by 2 h adsorption of the viral supernatants to the EPC cell monolayers, followed by washing the unbound viruses with infection media and incubation at their respective optimal replication temperatures during 24 h. The infected EPC cell monolayers were fixed and viral titers assayed by the *in vitro* by the focus forming units (ffu) assay as described before (Chinchilla et al., 2013b).

2.4. In vivo infections of adult zebrafish with VHSV, SVCV and bacteria

The procedures used for infecting zebrafish with VHSV or SVCV viruses were described before. Briefly, zebrafish were acclimatized to 14 °C for VHSV infection or to 22 °C for SVCV infection during 2 weeks

and infected for 2 h by bath immersion in cell culture supernatants containing 10^7 ffu/ml of VHSV (Estepa and Coll, 2015a) or 10^4 ffu/ml of SVCV(Garcia-Valtanen et al., 2017), respectively. Parallel, non-infected zebrafish were mock-infected with cell culture medium to calculate differential expression folds. Zebrafish infected at short times with rhabdoviruses were euthanized 2-days after infection. Zebrafish surviving rhabdovirus infections were euthanized 2 months after last infection of 2 consecutive VHSV infections, (Estepa and Coll, 2015a) or 1 month after SVCV infection (Encinas et al., 2013). Zebrafish surviving a chronic infection with *Aeromonas hydrophila* and *Vibrio fluvialis* as identified by the Microbiological Service of the Fundación Hospital Alarcon (Madrid Spain), were euthanized ~ 5 months after the first deaths were detected (Estepa and Coll, 2015a).

2.5. Harvest of lymphoid organs, fin tissues, and blood plasma from virally infected zebrafish

For microarray and RTqPCR studies, head kidney and spleen (lymphoid organs) and/or fin tissues were harvested and pooled from 3 zebrafish for each biological replica. Harvested samples for microarray/ RTqPCR analysis were kept in RNAlater (Qiagen) at −70 °C until used. For the proteomic studies, anesthetized zebrafish were bled by cutting the final end of their tails. Blood was collected in 100 μl of sterilized anticoagulant media (0.64 g sodium citrate, 0.15 g EDTA, 0.9 g sodium chloride per 100 ml of water containing 50 mg per ml of gentamicin) at 4 °C. Diluted blood was immediately centrifuged at 1000 g for 3 min to obtain plasma. Plasma were kept frozen at −70 °C until used.

2.6. Ethic statement on zebrafish handling

Zebrafish were handled following National and European guidelines. In addition, specific zebrafish protocols were locally approved by the Ethics Committee (authorization CEEA 2011/022) following the National Guidelines for type III experimentation (Annex X, permission RD53/2013). All personnel implicated in the handling of zebrafish obtained the special C National permission for training in animal experimentation. To record for health and behavior, the VHSV- or SVCV-infected fish were daily monitored 2-4 times. To minimize suffering (Huang et al., 2010), fish showing external haemorrhages and/or abnormal swimming behavior (endpoint criteria) were immediately euthanized by immersion in iced water (5 parts ice/1 part water, 0 − 4 °C) for 10 min and then exposed to an overdose of methanesulfonate 3-aminobenzoic acid ethyl ester (MS222, 300 mg/l) for > 10 min after cessation of opercular movement ("Guidelines for Use of Zebrafish in the NIH Intramural Research Program", http://oacu.od.nih.gov/ARAC/documents/Zebrafish.pdf). No fish died before meeting the endpoint criteria. MS222 at 90 mg/l was used to anesthetized the fish while obtaining blood. The fish were then euthanized by an overdose of MS222 to extract lymphoid organs and/or fin tissues.

2.7. RNA isolation from zebrafish tissues/organs and EPC cell monolayers

For RTqPCR tissues/organs analysis, RNA from different external tissues (fin, gill, gut) and internal organs (muscle, head kidney, spleen, liver) of healthy adult zebrafish were extracted and pooled from 4 individual zebrafish to obtain enough RNA. All tissues/organs were carefully dissected under a binocular loupe for each individual zebrafish by trained personnel. Tissues were excised and pooled from dorsal, ventral and caudal fins, while muscle was obtained from the tail part of the body and washed in PBS to avoid possible contamination with internal organs. For microarray analysis, pooled head kidney and spleen lymphoid organs or fins were pooled from 3-4 individual zebrafish for each biological replica to obtain enough RNA for hybridization. The pooled tissues/organs were immediately immersed in RNAlater (Ambion, Austin, USA) and maintained at 4 °C for 24 h before being frozen at −70 °C. RNA was extracted from sonicated samples (1 min x 3

times at 40 W in ice) using a commercial RNA isolation kit (RNeasy kit, Qiagen, Hilden, Germany) following manufacturer's instructions. For RTqPCR of EPC cell cultures, RNA from the cell monolayers were similarly extracted by the same RNeasy kit used above without the sonication step. Once purified, RNA concentrations were estimated by Nanodrop absorbances at 260 nm. The presence of 18 and 28 S RNA bands was confirmed by denatured RNA agar electrophoresis (Sigma, Che.Co, MS, USA). Purified RNAs were stored at −70 °C until used.

2.8. Estimation of relative expression of crp1-7 transcripts by RTqPCR

The 7 *crp* loci coding for 7 CRP isoform proteins, first identified in the CH211-234P6 linkage group 24 of the zebrafish (*Danio rerio*) genome (Falco et al., 2012), were used to define the 7 *crp1*/CRP1 to *crp7*/CRP7 (*crp1-7*/CRP1-7) transcript/protein isoform sequences and their corresponding specific probes and primers (Table S1). Reverse transcriptase quantitative polymerase chain reactions (RTqPCR) were performed to estimate *crp1-7* transcript levels. For that, one microgram of purified RNA from each sample was converted to its corresponding cDNA using RT from Moloney murine leukemia virus (Invitrogen) as previously described (Falco et al., 2008). Quantitative PCR (qPCR) was then performed using the ABI PRISM 7300 (Applied Biosystems, NJ, USA) with SYBR Green PCR master mix (Life Technologies, United Kingdom). Reactions were prepared in 20 μl volume with 2 μl of cDNA, 900 nM of each forward and reverse primers (Table S1) and 10 μL of SYBR Green PCR master mix. Non-template controls were included for each isoform analysis. The cycling conditions were 95 °C for 10 min, followed by 40 cycles at 65 °C 1 min, 95 °C for 1 min. The relative gene expression values were obtained using the $2^{-\Delta\Delta Ct}$ method (Livak and Schmittgen, 2001), by normalizing each *crp* gene expression value by the formula, expression of each gene/expression of *ef1a*.

2.9. Microarray hybridization and differential expression data analysis

Oligo probes of 60-mer and 80 ± 3 °C of melting temperature, specific for each of the zebrafish *crp1-7* sequences were designed (Array Designer 4.3, Premier Biosoft Palo Alto CA, USA) from the mRNA GenBank data base accession number sequences listed in Table S1 (accessed in 2013) as previously described (Estepa and Coll, 2015a). The *crp*1-7 oligo probes were included in the ID41401 and ID47562 home-designed immune-focused zebrafish microarray Agilents versions which were validated by RTqPCR in previous studies (Encinas et al., 2013; Estepa and Coll, 2015a). Both microarray designs were deposited also in the Gene Expression Omnibus (GEO) numbers GPL15747 and GPL17670, respectively. Extracted RNA samples from zebrafish tissues/organs were amplified and fluorescently labeled from 2 μg of high quality RNA (50 μg/ml) and hybridized to the above described microarrays by Nimgenetics (Cantoblanco, Madrid, Spain) as previously described (Encinas et al., 2013; Estepa and Coll, 2015a). Because genes previously classified as *saps* (Encinas et al., 2013) were recently identified as isoform variants of *crp2* (*sap1/sap2*) or *crp5* (*sap/sapp*) (Bello et al., 2017), their similar microarray expression data were included into the corresponding *crp* calculations. Raw data were normalized by the sum of all microarray fluorescences and outliers removed as described before in detail (Encinas et al., 2013; Estepa and Coll, 2015a). Raw and normalized data were deposited at GEO's GSE57952 (VHSV-infected and VHSV-/bacterial-survivor zebrafish), GSE58205 (SVCV-infected wild type zebrafish) and GSE54096 (*rag1-/-* mutant zebrafish) (Encinas et al., 2013; Estepa and Coll, 2015a; Garcia-Valtanen et al., 2017). Results were expressed in differential expression folds calculated by the formula detailed in each of the corresponding Figure legends (Figs. 1–3).
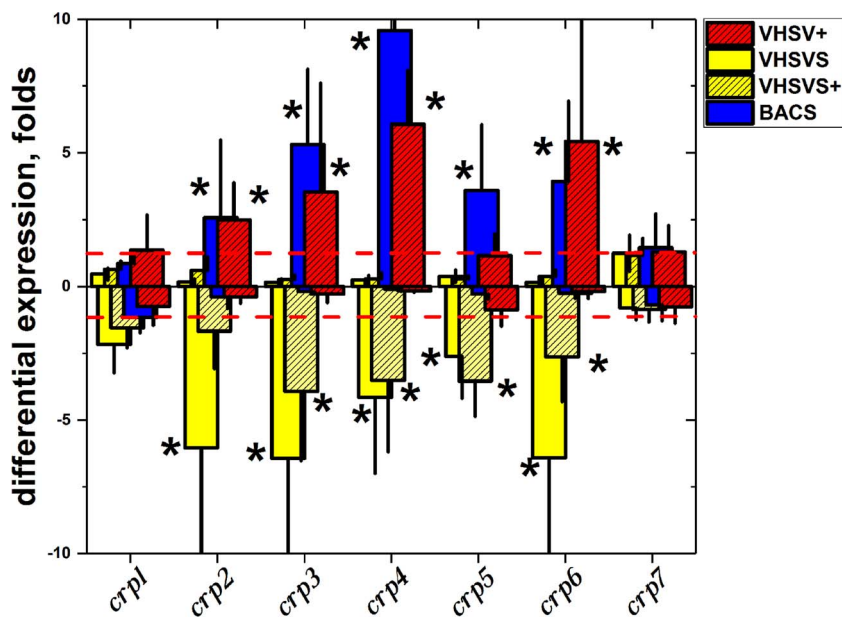
Fig. 1. Upregulated (positive bars) and downregulated (negative bars) *crp1-7* transcript profiles from lymphoid organs from zebrafish infected with VHSV (red) and surviving VHSV- (yellow) or bacterial- (blue) infections.

Fluorescence was assayed after hybridization of transcript samples from zebrafish organs to microarray *crp1-7* probes. Raw and normalized data were deposited in GEO's bank at GSE57952 (Estepa and Coll, 2015a). Differential expression folds (upregulated genes) were calculated by the formula, fluorescence of each gene from infected fish/mean fluorescence of each gene from non (mock)-infected fish. The same fold data were represented as the inverse folds and arbitrarily given a negative value (-1/folds) to best visualize the downregulated genes (duplicated representation). Using this type of duplicated representation, both positive (> 1.5 fold) and negative (< 0.66 fold = 1/1.5 fold) bars appeared in the positive and negative Y axes in the Figure. Outliers were removed and means and standard deviations represented (n = 4 replicas, 3 fish pooled per replica, total number of fish = 36). Only one of the ± standard deviations were represented to increase clarity. *, folds significatively > 1.5 (+, positive upregulated values) or < 0.66 (-, negative downregulated values) thresholds at p < 0.05 (Student t-test). **Red dashed horizontal lines**, 1.5- and 0.66-fold thresholds. **Red hatched bars,** 2-days after VHSV infection (VHSV +). **Open yellow bars,** 2-month VHSV-survivors (VHSVS). **Hatched yellow bars**, 2- days after VHSV re-infected 2-month VHSV-survivors (VHSVS +). **Blue bars**, 5-month *A. hydrophila*- and *V. fluvialis*-survivors (BACS).

2.10. Proteomic analysis of CRP1-7 induced by SVCV infection in zebrafish plasma

Adult zebrafish were infected with SVCV and their blood harvested after 0, 24, 48 and 120 h (5-days). Blood was obtained from 3 biological replicas for each time point, 3 fish pooled per replica (total amount of fish = 36). Red blood cells were immediately removed by centrifugation at 3000 g for 10 min at 4 °C. The resulting plasma samples were treated with 9 M urea, 2 M thiourea, 5% CHAPS (Dimethyl[3-(propyl). azaniumyl] propane-1-sulfonate), 2 mM TCEP (Tris(2-carboxyethyl) phosphine) and anti-protease cocktail (Sigma-Aldrich, St.Louis, Mi, USA). The samples were then precipitated with methanol/chloroform, quantified by the BCA assay (Pierce Protein Assay kit, Rockford, Il, USA) and digested with trypsin. The resulting peptides were cleaned using a StageTip-C18 column and 1 μg of each cleaned sample separated by liquid chromatography (LC) in a C-18 column employing a long gradient for elution to reduce hemoglobin-derived peptides. Mass spectrophotometry (MS) was performed in a Triple-TOF 6600 (LC/LC-MS/MS) Sciex apparatus (Framingham, MA, USA) at the Proteomic Facilities at the "Centro Nacional de Biotecnologia" (CNB, Cantoblanco, Madrid, Spain). The CRP1-7 protein accession numbers corresponding to the peptide sequences obtained were identified using the MASCOT search engine against the UNIPROT protein data base of zebrafish (*Danio rerio*). Only those CRP identified with more than 2 different peptides were considered for further analysis. Automatic CRP1-7 identifications were confirmed by manual comparison with sequences derived from mRNA accession numbers and/or blast against mRNA-derived protein sequence data banks. There were 1 to 5 UNIPROT accession numbers identified for each CRP isoform (Table S2) except for CRP6. The number of peptides, spectra counts, and peptide probability scores were used for quantitation of each of the CRP accession numbers identified. The results were finally normalized by the number of expected peptides per CRP1-7 using the emPAI method (Ishihama et al., 2005). Folds were then calculated by the formula, emPAI values of each CRP accession number at different times/emPAI mean value of each CRP accession number at time 0 (n = 3).

2.11. Preparation of pMCV1.4 plasmids coding for crp1-7

The pMCV1.4 plasmid was used for subcloning each of the *crp1-7* genes (accession numbers in Table S1). The MCV1.4 promoter is a large immediate early cytomegalovirus promoter which includes a synthetic intron to increase expression efficiency (Rocha et al., 2005). To obtain the plasmid constructs, the corresponding mRNA-derived *crp1-7* sequences were flanked by HindIII and XhoI restriction sites chemically synthesized, subcloned into pMCV1.4 and their resulting sequences confirmed by sequencing both strands (Genscript, NJ, USA). The resulting pMCV1.4-*crp1-7* plasmid constructs were used to transform *E.coli* DH5alpha by electroporation, amplified and isolated with the Endofree Plasmid Midi purification Kit (Qiagen, Germany) according to the manufacturer's instructions. Maximal concentrations of contaminating *E.coli* lipopolysaccharide (LPS) were estimated to be < 0.52 ng per 100 ng of purified plasmid according to the manufacturer. Purified plasmid solutions were adjusted to 1 mg/ml of total DNA (260 nm absorbances) which contained 80-100% of plasmid DNA, as shown by agarose gel electrophoresis. Purified plasmids were stored at −20 °C.

2.12. Transfection of EPC cell monolayers with pMCV1.4-crp1-7 and infection with Spring Viremia Carp Virus (SVCV)

EPC cell monolayers in 96-well plates (50000 EPC cells per well) in 100 μl of cell culture medium were transfected with 100 ng of each of the pMCV1.4-*crp1-7* plasmids complexed with 0.3 μl of FuGENE HD (Promega, Madison, WI, USA) for 24 h at 22 °C. Under these conditions, the transfection efficiency as determined by the percentage of fluorescent cells after transfection with pMCV1.4-*gfp* varied between 15 to 30% (n = 3 experiments). After transfection, the cell culture medium was removed, fresh medium added and 48 h later transcript expression estimated by RTqPCR as described above. When appropriated, the transfected EPC cell monolayers were infected with 50 focus forming units (ffu) of SVCV per well in 100 μl (multiplicity of infection of 10^{-3}) and incubated for viral adsorption for 2 h. Then the virus remaining in the supernatants were removed, fresh medium added and infected cell monolayers incubated for 24 h.

2.13. SVCV neutralization of pMCV1.4-crp1-7 plasmid transfected EPC cells or of CRP1-7-enriched supernatant-treated EPC cells

To study possible interference of CRP1-7 with SVCV replication in EPC cell monolayers, 2 types of *in vitro* micro-neutralization assays were performed. In the first type of assays, the EPC cell monolayers were transfected with pMCV1.4-*crp1-7* plasmids and 3-days later infected with SVCV as described above. The transcript expression levels relative

to the *ef1a* gen expression after transfection and before infection were similar for *crp1-7* (Fig. S1 A). In the second type of assays, large amounts of cell-free supernatants were obtained by transfecting EPC cell monolayers in multiple 96-wells with pMCV1.4-*crp1-7* and harvesting them 3-days later. Because Western blotting was not sensitive enough to detect the CRP presence in the supernatants, to concentrate CRP, 500 μl of supernatants had to be spotted onto each spot of the nitrocellulose filters. The CRP content of the concentrated CRP1-7 were estimated with anti-CRP rabbit antibodies raised against one of the most conserved carboxy-terminal amino acid stretches among zebrafish CRP1-7 ([189]DWDTIEYDVTGN) (GenScript, Piscataway, NJ, USA). To reduce background, the anti-CRP antibodies contained in the rabbit sera were purified by affinity chromatography on a mixture of DWDTIEYDVTGNGGGGGGKK/KKGGGGGGDWDTIEYDVTGN peptides coupled to CNBr-activated Sepharose. Affinity-purified anti-CRP antibodies bound to the CRP-enriched supernatant samples were detected with horseradish peroxidase labeled goat anti-rabbit immunoglobulins and ECL (BioRad) (Fig. S1 B). Further details of the method are given in Fig. S1 legend. To study the effects of CRP1-7-enriched supernatants, 100 μl were added to EPC cell monolayers for 24 h, washed, and monolayers infected with SVCV as indicated above.

In both types of assays, the number of infected EPC cells was determined by micro focus forming units (ffu) (n = 2 experiments) and flow cytometry (n = 2 experiments). The number of ffu were estimated by immunofluorescence of the fixed cell monolayers and staining with polyclonal anti-SVCV (BioX Diagnostics SA, Jemelle, Belgium) and rhodamine labeled goat anti mouse immunoglobulins (GAM-TRITC). The results were then expressed as percentage of neutralization calculated by the formula, 100 − (number of infected cells in transfected or treated EPC cells/number of infected cells in non-transfected or non-treated EPC cells). Flow cytometry was performed by the high throughput micro method (Chinchilla et al., 2013a). Briefly, SVCV-infected cell monolayers were fixed with formaldehyde, permeabilized with digitonine and stained with anti-SVCV (BioX Diagnostics SA, Jemelle, Belgium) and GAM-FITC. EPC cell suspensions were then obtained by trypsin digestion to be analyzed in a BD FACS Canto II apparatus (Beckton Dickinson, San Agustin de Guadalix, Madrid, Spain) provided with a high throughput sampler. The number of fluorescent cells (SVCV-infected cells) over a threshold containing 95% (mean + 2 standard deviations) of non-infected EPC cells was first determined. SVCV-infected cell monolayer controls in the absence of any treatment showed 25-40% of the EPC cells were infected depending on the experiment. The percentage of infected EPC cells was then calculated using the formula: 100 x number of cells with fluorescences above the threshold/total number of cells gated per well. The final results were expressed in % of neutralization by the formula: 100 − 100 x percentage of transfected or supernatant-treated and infected cells/percentage of infected cells in control cells. Because no significant differences were found between ffu and flow cytometry assays, their results were pooled and means and standard deviations calculated (n = 4).

To study possible interferences in the neutralization assays caused by *E.coli* LPS which could be contaminating the plasmids purified by the Endofree Plasmid Midi purification Kit (Qiagen, Germany), LPS from *E.coli* O55B5 and 0111:B4 strains (Sigma Che Co, St.Louis MS, USA) were added at different concentrations (20–500 ng per well) to non-transfected EPC cell monolayers. Those concentrations were higher than the estimated amounts which may be present when transfecting EPC cell monolayers with 100 ng of plasmids per well (< 0.52 ng per 100 ng of plasmid). The LPS-treated EPC cell monolayers were then infected with SVCV and finally assayed for neutralization by ffu (Fig. S2).

2.14. Injection of one-cell stage embryos with pMCV1.4-crp2-5 or pMCV1.4-il6 plasmids and resistance of zebrafish larvae to SVCV infection or induction of crp1-7 transcripts, respectively

To test for CRP1-7 induced resistance to SVCV, one-cell stage of zebrafish embryos were microinjected with 2 nl of phosphate buffered saline (PBS) containing 150 pg of pMCV1.4 plasmids coding for green fluorescent protein (GFP) and CRP2-5, by following the methodology described before (Pereiro et al., 2017). The microinjections were performed with pulled glass microcapillary pipettes (WPI, USA) and a Narishige IM-30 micromanipulator under an stereo microscope SMZ800 (Nikon). To study the effects of SVCV challenge, the resulting 3-day hatched larvae were anesthetized and 12 larvae per group were microinjected into the duct of Cuvier to induce a systemic infection with 2 nl of PBS containing 10^4 pfu of SVCV or only PBS per larvae. Results at each of the different times after infection were expressed in cumulative survival calculated by the formula 100 − (100 x number of dead fish injected with pMCV1.4-*gfp* or *crps*). A 64.5% mortality was obtained in fish injected with the pMCV1.4-*gfp* control 7 days after infection. Kaplan-Meier cumulative survival curves were analyzed for statistical significance with the log-Rank (Mantel-Cox) test (Mantel, 1966) by comparing the survival of fish injected with pMCV1.4-*crps* to those of pMCV1.4-*gfp*.

To test for the effects of IL6 on *crp1-7* expression, one-cell stage embryos were microinjected with 2 nl of PBS containing 150 pg of pMCV1.4 or pMCV1.4-*il6* plasmids as described above. Three-days later the larvae were pooled (n = 4 groups of 3 pooled fish per group, total number of larvae per group = 12), RNA extracted and *crp1-7* transcript levels evaluated by RTqPCR using the primers described in Table S1. Results were expressed relative to *ef1a* expression as calculated by the formula, 100 x *crp1-7* expression per group/*ef1a* expression per group. Means and standard deviations were represented.

2.15. Statistical analysis

Survival results represented by Kaplan-Meier survival curves were analyzed for statistically significance by the log-Rank (Mantel-Cox) test (Mantel, 1966) using the corresponding survival analysis feature of the computer software package OriginPro 2017 (64 bit, sr1) by comparing the survival of fish injected with pMCV1.4-*crps* to those of pMCV1.4-*gfp*, following previous reports (Pereiro et al., 2017). Results of microarray hybridization, RTqPCR and microneutralization were represented in differential expression folds or percentage of neutralization as the means ± standard deviation of n biological replicates. To determine their significant differences, the corresponding data were analyzed with OriginPro 2017 using Student's t-test. In the graphs, p < 0.05 significant differences were displayed as *.

3. Results

3.1. Levels of crp1-7 transcripts were specific of tissues and organs in healthy adult zebrafish

RNA from different external tissues (fin, gill, gut) and internal organs (muscle, head kidney, spleen, liver) of healthy adult zebrafish was extracted to investigate by RTqPCR the distribution of *crp1-7* transcript expression relative to the *ef1a* gene using specific primers (Table S1). Results showed amplified products corresponding to an average of 45.2 relative expression units for the 7 tissues and *crp1-7* isoforms. The *crp4/ crp6* in gills (Table 1A) and *crp3/crp5* in spleen (Table 1B) showed relative expressions ~3-6-fold higher (range from 124 to 293 relative expression units) than the average, while the expression of *crp3/crp5* in gills, *crp6* in gut, *crp4* in spleen and *crp2/crp3/crp4* in kidney were > 60 relative expression units (Table 1A, B in gray). On the contrary, *crp7* in all and *crp1* in some (fin, gut, spleen, liver) tissues/organs showed 10-50 lower expression levels than *crp2-6*. Each tissue/organ

Table 1

Levels of *crp1-7* transcripts in external tissues (A) and internal organs (B) of healthy adult zebrafish and their distribution in percentages (C).

Each of the total RNA from individual external tissues (**A**) or internal organs (**B**) from 4 adult zebrafish was RTqPCR amplified using the *crp1-7* specific primers listed in Table S1. The relative gene expression values were obtained using the $2^{-\Delta\Delta Ct}$ method. Each *crp1-7* gene expression value was normalized by the corresponding *ef1a* value by the formula, expression of each gene/expression of *ef1a*. Means (**bold**) and standard deviations (sd) were represented in Tables A and B (n = 4). Gray boxes, *crp* relative expression levels > 60. *, *crp* relative expression levels > 120. **C,** Pie *crp1-7* distribution in percentages of the total *crp* expression in each tissue/organ. **White pie**, *crp1*. **Green pie**, *crp2*. **Yellow pie**, *crp3*. **Dark-yellow pie**, *crp4*. **Red pie**, *crp5*. **Blue pie**, *crp6*. **Gray pie**, *crp7*.

A)

Transcript levels of *crp1-7* in external tissues of healthy adult zebrafish

crp	Fin	±sd	Gill	±sd	Gut	±sd
crp1	2.7	1.5	36.9	3.1	3.0	1.4
crp2	29.5	9.4	40.2	12.6	21.6	10.1
crp3	38.5	17.9	73.7	30.1	15.9	1.2
crp4	33.7	18.0	*149.3	47.6	28.5	15.8
crp5	25.8	11.3	67.1	30.0	34.3	34.9
crp6	25.0	12.8	*124.0	65.4	64.2	26.4
crp7	1.3	1.0	4.5	2.0	1.3	0.7

C)

FIN GILL GUT

Legend: CRP1, CRP2, CRP3, CRP4, CRP5, CRP6, CRP7
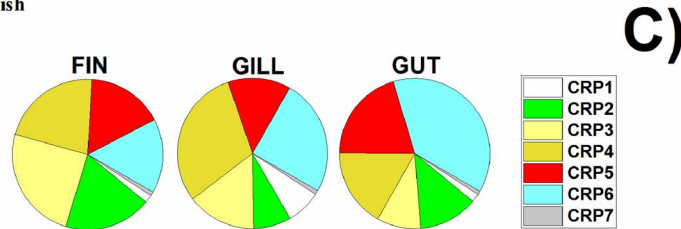
B)

Transcript levels of *crp1-7* in internal organs of healthy adult zebrafish

crp	Muscle	±sd	Head kidney	±sd	Spleen	±sd	Liver	±sd
crp1	17.8	10.2	32.0	20.4	5.6	4.3	4.22	3.0
crp2	56.2	20.6	63.4	26.5	50.3	14.3	34.06	7.3
crp3	26.3	18.4	66.3	31.4	*191.8	109.0	42.74	7.4
crp4	42.2	21.9	95.1	16.9	65.9	12.4	50.01	21.0
crp5	55.3	57.4	57.4	46.7	*293.2	89.8	29.88	5.9
crp6	30.5	2.9	30.1	18.1	34.4	22.1	44.68	1.5
crp7	2.3	1.3	1.7	1.5	0.6	0.5	1.04	0.7

MUSCLE KIDNEY SPLEEN LIVER
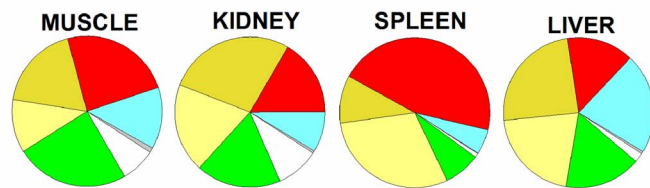
had a different distribution of constitutive *crp1-7* expression levels when expressed in percentage of their total expression (Table 1C). For instance, *crp5* was the most abundant in percentage in spleen and was present at relatively high levels in most tissues/organs while *crp2* was most abundant in muscle/head kidney and *crp6* in gut/gill/liver (Table 1C). A similar tissue/organ specificity was already described in common carp for its *crp1-2* isoforms (Falco et al., 2012). The existence of tissue-specific distribution of *crp1-7* transcript levels suggested different functionalities among the 7 zebrafish CRP isoforms. Therefore, to study whether or not the constitutive levels of *crp1-7* transcripts in healthy zebrafish tissues/organs may change after infection, head kidney plus spleen (the most important lymphoid internal organs) and fins (the easiest-to-obtain external tissue) were selected for further experimentation.

3.2. Zebrafish infected with VHSV or surviving VHSV/bacterial infections showed heterogeneous changes in the differential expression of their crp1-7 transcripts in lymphoid organs

Hybridization values (fluorescent arbitrary units) and differential expression folds (infected *versus* non-infected zebrafish) of *crp1-7* transcripts from lymphoid organs were explored by microarray hybridization using a unique home-designed platform which included 7 *crp* (*crp1-7*) specific probes (Table S1, Fig. 1).

In all the infection/survival situations studied, the hybridization values varied from 1 to 30000 fluorescent arbitrary units. However, while the *crp2-6* values ranged from 1000 to 30000 units, all *crp1* values ranged from 1 to 50 and those of *crp7* from 10 to 200 units (not shown). Therefore, the constitutive expression levels of *crp1/crp7* found in healthy zebrafish tissues/organs (Table 1) remained low after viral or bacterial infections when compared to the rest of *crp2-6*.

When expressed as differential expression folds, the results showed that after VHSV-infection *crp2/crp3/crp4/crp6* were upregulated (2-5-fold), while *crp1/crp5/crp7* remained unmodulated (Fig. 1, positive red

hatched bars). Similar results were obtained for bacterial survival, although their corresponding upregulation levels were higher (Fig. 1, positive blue bars). However, in bacterial survival, *crp5* was also upregulated (Fig. 1, positive *crp5* blue bar), suggesting that *crp5* responses may differentiate bacterial from viral infections. The upregulation of zebrafish *crp2-6* isoforms resembled that of human pCRP after bacterial infection/survival (Kindmark, 1971). In conclusion, the profile of zebrafish *crp1-7* modulation was comparable between bacterial survival and viral infections, except for *crp5*.

In contrast to viral infection and bacterial survival, fish surviving VHSV infection (VHSV-survivors) resulted in downregulated levels of *crp2-6* (Fig. 1, negative yellow bars). The levels of *crp1/crp 7* remained unmodulated. After VHSV re-infection of the VHSV- survivors, the levels of *crp2/crp3/crp6* increased but still remained downregulated (compare negative yellow empty with yellow hatched bars in Fig. 1).

3.3. Fins showed higher differential expression levels of crp2-6 than lymphoid organs after SVCV-infection and in SVCV-survivors

The *crp1-7* transcriptional profiles were comparatively studied in internal lymphoid organs and external fin tissues. Differential expression folds showed that after SVCV-infection, only *crp4/crp7* in internal lymphoid organs were slightly upregulated (Fig. 2A, white hatched bars), while in external fins, *crp2/crp4/crp5* were upregulated, specially *crp5* (~ 7-fold) (Fig. 2A, gray hatched bars). Similarly, in SVCV-survivors, *crp2/crp4/crp5* in lymphoid organs were slightly upregulated (Fig. 2B, white hatched bars), while in fins, *crp2-6* increased their upregulation, specially *crp5* (> 15-fold) (Fig. 2B, gray hatched bars).

3.4. Lymphoid organs from adaptive-deficient rag1⁻/⁻ zebrafish mutants showed high levels of differential expression of crp1-6 when infected with SVCV

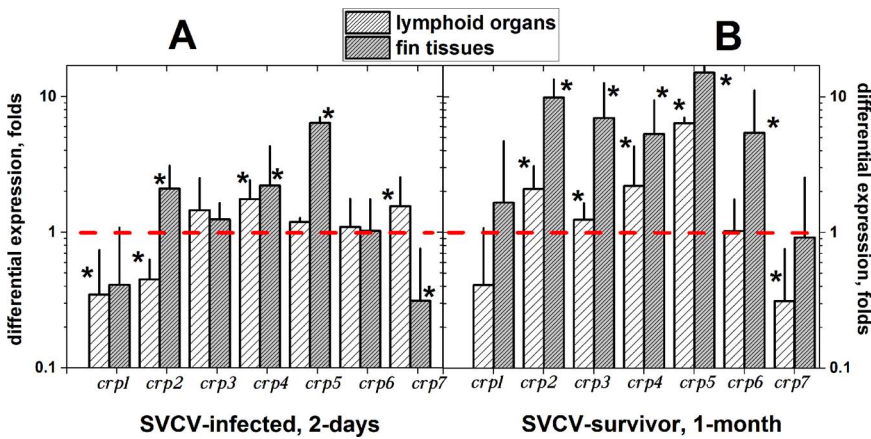To explore any possible relation between *crp* and adaptive immunity

negative hatched bar). The *crp2/crp5* showed the highest upregulated levels (~ 10 and 17-fold, respectively) in the absence of adaptive immunity.

3.5. Time course of CRP1-7 protein differential expression in zebrafish plasma after SVCV infection

To compare *crp1-7* transcript levels in lymphoid organs with CRP1-7 protein levels in blood after SVCV infection, we followed the time course of different CRP UNIPROT accession numbers by double liquid chromatography/mass spectrophotometry (LC/LC/MS/MS) in plasma samples from SVCV-infected zebrafish. Because of the similarity of amino acid sequences among zebrafish CRP1-7 isoforms (Bello et al., 2017), the CRP1-7 identifications derived from the tryptic peptide analysis should be taken with caution. For instance, some of the peptides could not differentiate between CRP2/CRP3, some peptides were common to CRP2 and CRP6, and no unique CRP6 peptides could be detected. Despite those limitations, after 24 h, the number of accession numbers and the differential expression folds were higher in several of the CRP2/CRP5 than in CRP3/CRP4. After 48 h, only CRP2 showed one higher fold than all the rest of CRPs which were similar or lower than their levels at time 0 (fold = 1). After 120 h, all identified CRPs were lower than their levels at time 0 (Fig. 4). The evolution of all CRP plasma levels in zebrafish after SVCV infection were similar to those reported in carp CRP after infection with herpesvirus (Pionnier et al., 2014).

In conclusion, the *crp2*/CRP2 and *crp5*/CRP5 were among the most important isoforms participating in zebrafish viral responses, as suggested by most of the results obtained from the tissue/organ-specificity of *crp1-7* levels on healthy zebrafish (Table 1), the *crp1-7* expression in lymphoid organs of fish infected/surviving VHSV/bacterial infections (Fig. 1), the comparative studies of *crp1-7* transcripts from organs/fins after SVCV infection (Fig. 2), the *crp1-7* highest expression on adaptive-deficient mutants infected with SVCV (Fig. 3) and the plasma levels of CRP1-7 proteins after SVCV infection (Fig. 4). In contrast, *crp1*/CRP1 and *crp7*/CRP7 remained unmodulated in most of the infection situations mentioned above. On the other hand, since all those *in vivo crp1-7*/CRP1-7 responses could be due to some interference with viral replication, we next undertook a series of experiments focusing on neutralization assays.

3.6. Fish cells transfected with pMCV1.4-crp1-7 or treated with CRP1-7-enriched supernatants neutralized SVCV

To investigate possible interferences of zebrafish *crp1-7*/CRP1-7 with SVCV replication, *crp1-7* mRNA sequences were cloned into the pMCV1.4 eukaryotic expression plasmid. Micro-neutralization assays for SVCV infection were then performed after using two complementary
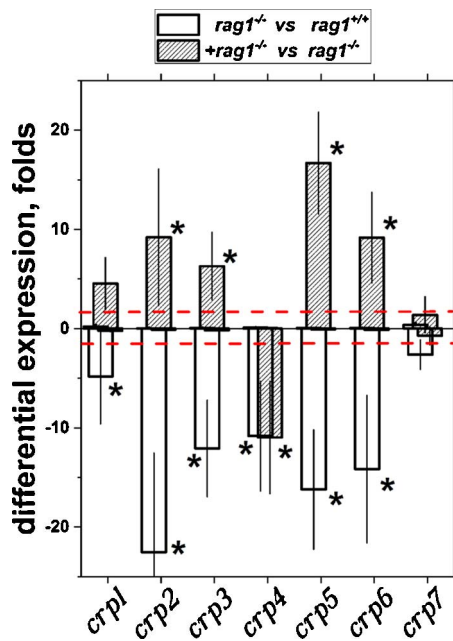

Fig. 3. Upregulated (positive bars) and downregulated (negative bars) *crp1-7* transcript profiles from lymphoid organs from $rag1^{-/-}$ mutants before and after SVCV infection. Differential expression folds and standard deviations were calculated by the formula, fluorescence of each gene from $rag1^{-/-}$ mutant fish/mean fluorescence of each gene from $rag1+/+$ fish (white bars) and fluorescence of each gene from SVCV-infected $rag1^{-/-}$ mutants/mean fluorescence of each gene from $rag1^{-/-}$ mutant fish (hatched gray bars). The upregulated and downregulated results were represented as the duplicated representation explained in Fig. 1. Raw and normalized data were deposited in GEO's bank at GEO's GSE54096 (Garcia-Valtanen et al., 2017). *, folds significatively > 1.5 (+, positive upregulated values) and < 0.66 (-, negative downregulated values) at $p < 0.05$ (Student t-test). **Red dashed horizontal lines**, 1.5- and 0.66-fold thresholds. **White bars,** $rag1^{-/-}$ versus $rag1^{+/+}$ genotypes, n = 2 replicas each, 3 fish pooled per replica ($rag1^{-/-}$ vs $rag1^{+/+}$). **Hatched gray bars**, 2-day SVCV-infected $rag1^{-/-}$ phenotype versus 2-day mock-infected $rag1^{-/-}$ genotype, n = 2 replicas each, 3 fish pooled per replica (+$rag1^{-/-}$ vs $rag1^{-/-}$).

responses, the *crp1-7* responses to viral infection (innate responses) were studied in the absence of adaptive immunity ($rag1^{-/-}$ mutants) and compared to wild type $rag1^{+/+}$ mutants. In addition, *crp1-7* transcripts were analysed in lymphoid organs from zebrafish $rag1^{-/-}$ mutants without (mock infected) and after infection with SVCV. Results showed that compared to wild type $rag1^{+/+}$, the *crp1-6* were 5-20-fold downregulated in $rag1^{-/-}$ mutants (Fig. 3, negative empty bars). In sharp contrast, highly upregulated levels of *crp1-6* appeared 2-days after the $rag1^{-/-}$ mutants were infected with SVCV compared to mock-infected $rag1^{-/-}$ mutants (Fig. 3, positive hatched bars), except for *crp4* which remained similarly downregulated in both cases (Fig. 3,
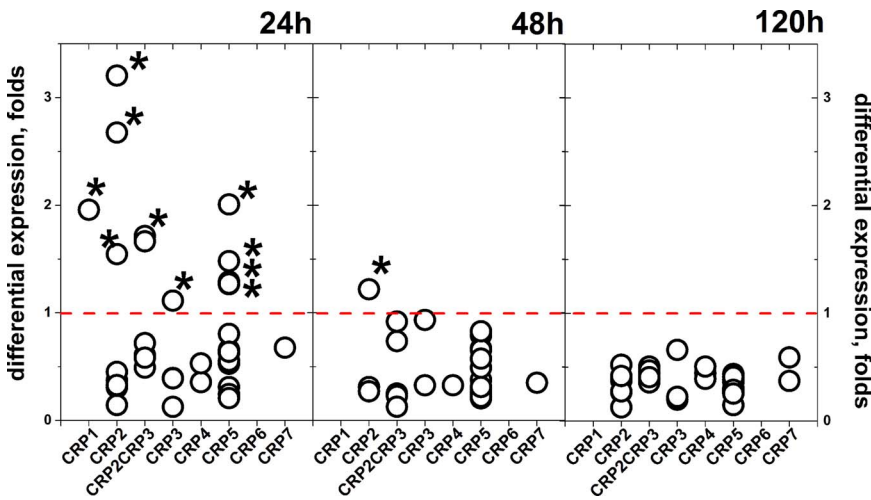
Fig. 4. Differential expression of CRP1-7 UNIPROT accession numbers in blood plasma from SVCV-infected zebrafish. Plasma was harvested from zebrafish infected with SVCV at different time points (0, 24, 48 and 120 h). For the calculations, 3 biological replicas were analyzed per time point. Each replica consisted in pools of 3 plasma (total number of fish = 36). Pooled plasma proteins for each replica were digested with trypsin, the resulting peptides separated by LC and analysed in a Triple-TOF (LC-MS/MS) apparatus. Table S2 shows that there were 1-5 UNIPROT accession numbers identified for each of the CRP1-7 isoforms. After emPAI normalization, differential expression folds were calculated by the formula, emPAI values of each UNIPROT accession number/emPAI mean value of the corresponding UNIPROT accession number at time 0. **Open circles**, folds of each of the UNIPROT accession numbers detected in the 3 replicas per time point. *, folds significatively > 1 at $p < 0.05$ (Student t-test). **Red dashed horizontal line**, 1-fold threshold. CRP6 was not identified by any of the peptides obtained.

strategies to deliver *crp1-7*/CRP1-7 to fish cells *in vitro*, i) transfection of EPC cell monolayers with pMCV1.4-*crp1-7* or ii) treatment of EPC cell monolayers with CRP1-7-enriched supernatants obtained from pMCV1.4-*crp1-7*-transfected EPC cells. To interpret possible differences of expression among the CRP isoforms, the efficiency of transfection of each of the pMCV1.4-*crp1-7* plasmid constructs and the presence of each of the corresponding CRP1-7 proteins in the supernatants were first studied by RTqPCR and dot-blot, respectively. Results showed that no significative differences could be demonstrated between relative expression levels of *crp1-7* transcripts in pMCV1.4-*crp1-7* transfected cells (Fig. S1, A). On the other hand, despite their low level of protein expression (i.e., when compared to CRP levels in zebrafish intraperitoneal ascites), prevented any quantitative analysis, CRP1-7 were present in enriched supernatants from pMCV1.4-*crp1-7* transfected cells (Fig. S1, B). In contrast no stained spot could be obtained in supernatants from pMCV1.4-*gfp* transfected cells (Fig. S1, B, lane 8). On the other hand, since bacterial LPS traces contaminating the pMCV1.4-*crp1-7* plasmid preparations could be causing also neutralization, LPS from *E.coli* were added to the cells and neutralization measured. No neutralization effects on SVCV infectivity could be demonstrated even at the highest LPS concentrations tested (~1000-fold higher than those expected to be present in the plasmids) with any of the two different sources of LPS (Fig. S2). In contrast, parallel assays with cells transfected with pMCV1.4-*crp2/crp5*, confirmed, once more, the neutralization of SVCV (Fig. S2). Therefore, only sequence and/or conformational differences among the CRP1-7 isoforms could be responsible for inducing neutralization of SVCV.

Results showed that the SVCV neutralization profiles obtained by transfecting EPC cells with the pMCV1.4-*crp1-7* plasmids were similar to those obtained by treating the cells with the CRP1-7-enriched supernatants (Fig. 5A and B, respectively). Thus, *crp2*/CRP2*, crp3* and *crp5*/CRP5 obtained maximal neutralization values of ~ 65-75% in both transfected and treated cells, respectively (Fig. 5A and B). Lower but significant neutralization percentages (~ 35-65%) were obtained for CRP3, *crp4*/CRP4*, crp6*/CRP6 and *crp7*/CRP7. In contrast, no neutralization was obtained when using *crp1*/CRP1 (< 7%).

Co-transfections were used to study possible neutralization synergies among *crp1-7*/CRP1-7. Synergy was defined as the increase in neutralization levels when co-transfecting two (pMCV1.4-*crp*^{a} + pMCV1.4-*crp*^{b}) rather than one pMCV1.4-*crp1-7* plasmid. To carry out co-transfections, the concentration of each plasmid was reduced from 100 to 50 ng per well. When required, 50 ng per well of the pMCV1.4-*gfp* plasmid were added to obtain the same final concentration of 100 ng of DNA per well (pMCV1.4-*crp* + pMCV1.4-*gfp*). Results of several co-transfections with different combinations between two pMCV1.4-*crp1-7* plasmids showed that the neutralization levels were
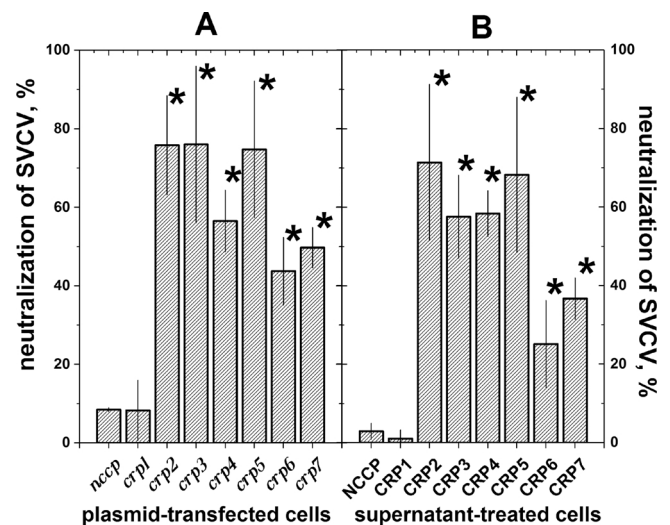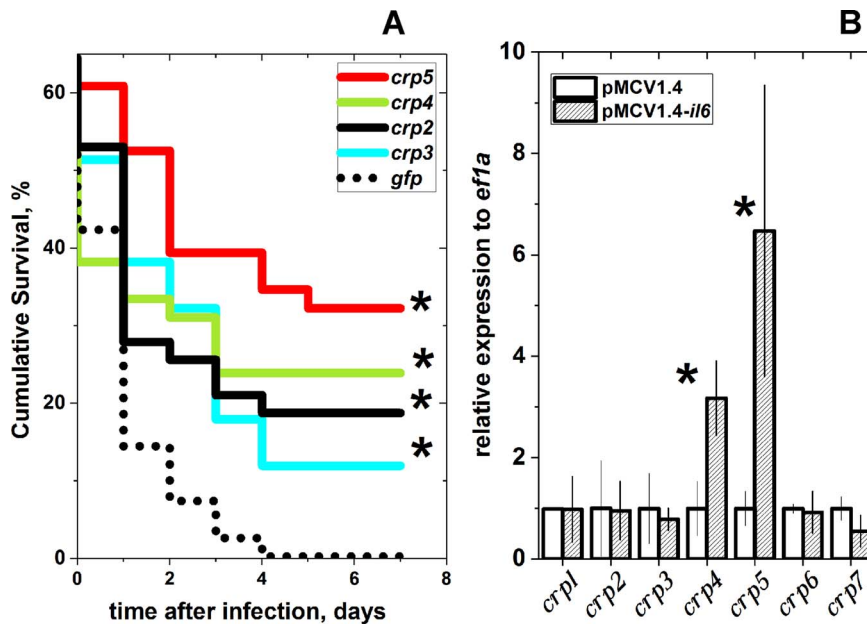

Fig. 5. Neutralization of SVCV in pMCV1.4-*crp1-7* plasmid-transfected EPC cells (A) or in CRP1-7-enriched supernatant-treated EPC cells (B).
A) EPC cell monolayers transfected with pMCV1.4-*crp1-7* plasmids. Cells were transfected with pMCV1.4-*crp1-7* plasmids and incubated for 3 days before SVCV infection (3-day exposure to *crp1-7*). **B) EPC cell monolayers treated with CRP1-7-enriched supernatants**. Cells were treated with CRP1-7-enriched supernatants (obtained from pMCV1.4-*crp1-7* transfected EPC cells) during 24 h before SVCV infection (1-day exposure to CRP1-7). To infect with SVCV, the transfected/treated cell monolayers were incubated during 2 h with SVCV, washed and incubated during 24 h. The number of SVCV infected EPC cells were then determined by ffu assays (n = 2 experiments) or flow cytometry (n = 2). Results from the 2 methods were pooled to calculate means and standard deviations (n = 4). The results were expressed as neutralization percentages calculated by the formula, 100 − (number of SVCV infected cells in transfected or treated cells/number of SVCV infected cells in non-transfected or non-treated cells). *, statistically higher than neutralization levels obtained from cells transfected with pMCV1.4 (no CRP-coding plasmid, *nccp*) or treated with the corresponding supernatants (NCCP) at $p < 0.05$ (Student t-test).

always lower (Fig. S3, hatched bars) than the theoretical sum obtained when the plasmids were separately transfected (Fig. S3, black horizontal bars). These results suggested some kind of interferences rather than synergies at the transcript or at the protein levels between *crp1-7*/CRP1-7 isoforms. Interferences could be due to the formation of neutralization-inactive CRP heteropolymers, to *crp* transcriptional controls or to changes in viral specificity (since they could still neutralize other viruses). Further work needs to be done to explore such possibilities.

In conclusion, all the above mentioned results suggested that zebrafish *crp2-7*/CRP2-7 (all except *crp1*/CRP1) neutralized SVCV *in vitro*.

Fig. 6. Study of the larvae from injected one-cell stage zebrafish embryos: injection of pMCV1.4-*crp2-5* and survival after infection with SVCV (A), and injection of pMCV1.4-*il6* and induction of *crp1-7* transcripts (B).

A) Five groups of 30 one-cell stage embryo per group (total number = 150) were intraperitoneally microinjected with 2 nl of phosphate buffered saline (PBS) containing 150 pg of pMCV1.4 plasmids coding for green fluorescent protein (GFP) or CRP2-5. Three days later, 12 hatched larvae per group were microinjected into the duct of Cuvier to induce a systemic infection with 10^4 pfu of SVCV resulting in 64.5% mortality for pMCV1.4-*gfp* injection after 7 days. Kaplan-Meier cumulative survival curves were analyzed for statistical significance with a log-Rank (Mantel-Cox) test (Mantel, 1966) as described before (Pereiro et al., 2017). *, Significative differences between survival of fish injected with pMCV1.4-*crps* and those injected with pMCV1.4-*gfp* at the p < 0.05 level. **Black dotted line,** pMCV1.4-*gfp*. **Red line,** pMCV1.4-*crp5*. **Black line,** pMCV1.4-*crp2*. **Blue line,** pMCV1.4-*crp3*. **Green line**, pMCV1.4-*crp4*. **B)** One-cell stage embryos were intraperitoneally microinjected with 2 nl of PBS containing 150 pg of pMCV1.4 or pMCV1.4-*il6* plasmids. Three-days later the corresponding larvae were pooled (n = 4 groups of 3 pooled fish per group, total number of larvae per group = 12), RNA extracted and *crp1-7* transcript levels estimated by RTqPCR using the primers described in Table S1. Results were expressed relative to *ef1a* as calculated by the formula, 100 x (*crp1-7* expression per group/*ef1a* expression per group). Means and standard deviations were represented. *, statistically higher than the mortality levels obtained after transfection with the pMCV1.4 plasmid at p < 0.05 (Student t-test). **Open bars,** injected with pMCV1.4. **Hatched bars**, injected with pMCV1.4-*il6*.

3.7. Microinjection of zebrafish embryos with pMCV1.4-crp2-5 induced protection to SVCV infection and injection of pMCV1.4-il6 induced crp4-5 transcripts

To investigate whether or not the *in vitro* neutralization of SVCV by *crp1-7*/CRP1-7 could be also observed *in vivo*, selected pMCV1.4-*crp2-5* plasmids were microinjected into one-cell stage zebrafish embryos. Three days later, the hatched larvae were challenged by microinjection of 10^4 pfu of SVCV per larvae. The cumulative survivals obtained after 7 days of SVCV challenge for the fish injected with the pMCV1.4-*crp2-5* plasmids were ~ 18, 12, 24 and 32%, respectively (Fig. 6A) in contrast to 0% of those injected with pMCV1.4-*gfp*.

Because mammalian *il6* is one of the major physiological inducers of CRP synthesis (Du Clos and Mold, 2011), and IL6 was upregulated after mammalian viral infections (Paludan, 2001; Wang et al., 2015; Xia et al., 2015), we tested also whether the microinjection of pMCV1.4-*il6* into zebrafish egg embryos modulated *crp1-7* expression in the resulting larvae. Results showed that only *crp4-5* were upregulated in larvae after injection of pMCV1.4-*il6* in zebrafish egg embryos (Fig. 6B).

4. Discussion

Several correlations and evidences for *in vitro* and *in vivo* viral neutralizing heterogeneous activities of zebrafish CRP1-7 isoforms were presented here. Previous observations included correlations between zebrafish CRP-related pathways and viral infections with either SVCV (Encinas et al., 2013) or VHSV (Estepa and Coll, 2015a). On the other hand, the Ca^{++}-dependent phospholipid-binding pocket structures of *in silico*-modelled CRP1-7 using the CRP5 3D X-ray structure as template, suggested the existence of a functional heterogeneity (Chen et al., 2015). The present work characterized and extended those previous observations to the different distributions of *crp1-7* transcripts in healthy tissues/organs and the heterogeneous *crp1-7*/CRP1-7 responses during several *in vivo* viral infections. Unexpected evidences for both *in vitro* neutralization and *in vivo* protection against viral infection of some but not all *crp1-7*/CRP1-7 isoforms were then demonstrated.

To our knowledge, this work is the first to report both *in vitro* neutralization and *in vivo* protection of viral infection by any CRP. However, the corresponding mechanism(s) underlying these effects are

not yet known. Different CRP1-7 conformations (Braig et al., 2017; Eisenhardt et al., 2009a; Eisenhardt et al., 2009b; Li et al., 2016; Wang et al., 2011; Wu et al., 2015), heterologous trimers (Bello et al., 2017), interferences with low-pH induced rhabdoviral fusion (Estepa and Coll, 1996; Estepa et al., 2001), and/or interactions of CRP1-7 carboxy-terminal domains (Potempa et al., 2015; Wang et al., 2011)(Li et al., 2016; Wu et al., 2015) or derived peptides (El Kebir et al., 2011; Shephard et al., 1989; Yavin and Fridkin, 1998) with lipid membranes including cholesterol-enriched lipid rafts, may offer possible mechanisms for the viral neutralization by CRP1-7. Alternatively or simultaneously, *crp1-7*/CRP1-7 molecules could also differentially interact with infected or uninfected cells to induce other yet unknown isoform-specific innate immunity defenses. Future work should be focused on some of the above mentioned possibilities to find a suitable explanation for the heterogeneous anti-viral activities induced by zebrafish *crp1-7*/CRP1-7.

The physiological mechanism through which the injection of pMCV1.4-*crp2-5* to egg embryos induced protection of larvae against SVCV challenge is also unknown. Once translated into proteins and after reaching the blood, it is supposed that the tested circulating CRP2-5 would be transported by the blood to target SVCV and/or SVCV-infected cells. After binding to exposed phospholipid heads in SVCV-damaged cells, CRP could induce inflammatory stimulus (i.e., *il6, il1b*). At this respect, it seems to be confirmatory that *crp5* was induced by injection of *il6*, a cytokine that upregulates circulating pCRP in humans (Du Clos and Mold, 2011) and is itself upregulated by viral infections (Paludan, 2001; Wang et al., 2015; Xia et al., 2015). Although nothing is known about zebrafish CRP1-7-ligand functionality, these isoforms may behave like in humans which bind C1q (increasing complement-aided cell lysis) and/or immunoglobulin FcR (increasing phagocytosis of tagged cells). On the other hand, cell migration from lymphoid organs to external tissues may explain downregulation of most *crp2-6* levels in survivors of viral infection and in *rag1*$^{-/-}$ mutants. The higher upregulation of *crp2/crp3/crp5* in fins compared to that in lymphoid organs (*crp2-6*) after SVCV infection and in SVCV survivors may confirm that hypothesis. While these results correlate with the elevated numbers of leukocytes in *rag1*$^{-/-}$ zebrafish external tissues (Garcia-Valtanen et al., 2017), the depletion of lymphoid organ IgM$^+$ cells despite the presence of neutralizing antibodies in plasma from VHSV-

survivor zebrafish (Estepa and Coll, 2015a), the trans endothelial leukocyte migration visually observed on zebrafish transparent larvae during viral infection (Varela et al., 2014) and/or the leukocyte cell migration during other zebrafish diseases (Deng and Huttenlocher, 2012), additional evidence should be provided to confirm cell migration when specific cellular reagents will become available for zebrafish. All these possible *in vivo* mechanisms remain to be investigated.

Despite the different experimental approaches, *crp2*/CRP2 and *crp5*/CRP5 were among the major actors in most anti-viral responses, while very often *crp1*/CRP1 and *crp7*/CRP7 remained unmodulated, and *crp3*/CRP3, *crp4*/CRP4, *crp6*/CRP6 were only modulated in some cases. On the other hand, *in vitro* assays demonstrated that *crp2*/CRP2 and *crp5*/CRP5 neutralized SVCV infectivity to the highest extent. In addition, *in vivo* injection of pMCV1.4-*crp2-5* confirmed that *crp5*/CRP5 was the most important contributor to survival of zebrafish larvae to SVCV challenge and one of the unique *crp*/CRP that together with *crp4*/CRP4 could be induced by injection of *il6* (a well known inducer of pCRP synthesis in humans). The low participation of CRP1 (the only zebrafish CRP lacking signal peptide) in viral responses and neutralization, suggested the idea that CRP2-7 should be secreted to be efficient. However, since CRP1 levels were detected also in CRP1-enriched supernatants, other explanation(s) may be possible. The lack of generation of CRP1 anti-viral peptides may offer an alternative explanation. Thus, because of the presence in CRP2-7 of a protease-sensitive site ([146]SFN or SFD) which is not totally conserved in CRP1 ([146]DFE) (Bello et al., 2017), such hypothetically neutralizing peptides may be derived from all CRPs except from CRP1. The lack of differential expression of *crp7*/CRP7 has no similar possible explanations, since it has signal peptide, identical protease site sequence than other CRPs and some anti-viral neutralization capacity. One possible explanation for the absence of differential expression may be that *crp7*/CRP7 could be induced in response to other pathogen infections (i.e., parasites?) and/or physiological conditions (i.e., other kind of tissue damage or internal stimulus, etc). The different experimental approaches, different fish used for the experiments, and confirmation of some results at 3 different laboratories, argue in favour of the existence of functional heterogeneity among *crp1-7*/CRP1-7 isoforms.

Zebrafish might provide a suitable model for further *crp1-7*/CRP1-7 studies. For instance, ligand-CRP1-7-binding specificities could be explored to define whether isoform heterogeneity may be related to a wider anti-viral functionality in the aquatic environment.

Acknowledgements

Appendix A. Supplementary data

Supplementary data associated with this article can be found, in the online version, at http://dx.doi.org/10.1016/j.molimm.2017.09.005.

References

Adinolfi, L.E., Zampino, R., Restivo, L., Lonardo, A., Guerrera, B., Marrone, A., Nascimbeni, F., Florio, A., Loria, P., 2014. Chronic hepatitis C virus infection and atherosclerosis: clinical impact and mechanisms. World J Gastroenterol 20, 3410–3417.

Ahne, W., Bjorklund, H.V., Essbauer, S., Fijan, N., Kurath, G., Winton, J.R., 2002. Spring viremia of carp (SVC). Diseases of Aquatic Organisms 52, 261–272.

Ashraf, U., Lu, Y., Lin, L., Yuan, J., Wang, M., Liu, X., 2016. The spring viremia of carp virus: recent advances. J Gen Virol.

Ballesteros, N.A., Saint-Jean, S.S., Encinas, P.A., Perez-Prieto, S.I., Coll, J.M., 2012. Oral immunization of rainbow trout to infectious pancreatic necrosis virus (Ipnv) induces different immune gene expression profiles in head kidney and pyloric ceca. Fish Shellfish Immunol 33, 174–185.

Bello, M., Falco, A., Medina, R., Encinar, J.A., Novoa, B., Perez, L., Estepa, A., Coll, J., 2017. Structure and functionalities of the human c-reactive protein compared to the zebrafish multigene family of c-reactive-like proteins. Developmental & Comparative Immunology 69, 33–40.

Boshra, H., Li, J., Sunyer, J.O., 2006. Recent advances on the complement system of teleost fish. Fish Shellfish Immunol 20, 239–262.

Braig, D., Nero, T.L., Koch, H.G., Kaiser, B., Wang, X., Thiele, J.R., Morton, C.J., Zeller, J., Kiefer, J., Potempa, L.A., Mellett, N.A., Miles, L.A., Du, X.J., Meikle, P.J., Huber-Lang, M., Stark, G.B., Parker, M.W., Peter, K., Eisenhardt, S.U., 2017. Transitional changes in the CRP structure lead to the exposure of proinflammatory binding sites. Nat Commun 8, 14188.

Chen, R., Qi, J., Yuan, H., Wu, Y., Hu, W., Xia, C., 2015. Crystal structures for short-chain pentraxin from zebrafish demonstrate a cyclic trimer with new recognition and effector faces. J Struct Biol 189, 259–268.

Chinchilla, B., Encinas, P., Estepa, A., Coll, J.M., Gomez-Casado, E., 2013a. Optimization of fixed-permeabilized cell monolayers for high throughput micro-neutralizing antibody assays: Application to the zebrafish/viral haemorragic septicemia virus (VHSV) model. Journal Virological Methods 193, 627–632.

Chinchilla, B., Gomez-Casado, E., Encinas, P., Falco, A., Estepa, A., Coll, J., 2013b. In vitro neutralization of viral haemorrhagic septicemia virus (VHSV) by plasma from immunized zebrafish. Zebrafish 10, 43–51.

Deng, Q., Huttenlocher, A., 2012. Leukocyte migration from a fish eye's view. J Cell Sci 125, 3949–3956.

Du Clos, T.W., Mold, C., 2011. Pentraxins (CRP, SAP) in the process of complement activation and clearance of apoptotic bodies through Fcgamma receptors. Curr Opin Organ Transplant 16, 15–20.

Eisenhardt, S.U., Habersberger, J., Murphy, A., Chen, Y.C., Woollard, K.J., Bassler, N., Qian, H., von Zur Muhlen, C., Hagemeyer, C.E., Ahrens, I., Chin-Dusting, J., Bobik, A., Peter, K., 2009a. Dissociation of pentameric to monomeric C-reactive protein on activated platelets localizes inflammation to atherosclerotic plaques. Circ Res 105, 128–137.

Eisenhardt, S.U., Habersberger, J., Peter, K., 2009b. Monomeric C-reactive protein generation on activated platelets: the missing link between inflammation and athero-thrombotic risk. Trends Cardiovasc Med 19, 232–237.

El Kebir, D., Zhang, Y., Potempa, L.A., Wu, Y., Fournier, A., Filep, J.G., 2011. C-reactive protein-derived peptide 201-206 inhibits neutrophil adhesion to endothelial cells and platelets through CD32. J Leukoc Biol 90, 1167–1175.

Encinas, P., Garcia-Valtanen, P., Chinchilla, B., Gomez-Casado, E., Estepa, A., Coll, J., 2013. Identification of multipath genes differentially expressed in pathway-targeted microarrays in zebrafish infected and surviving spring viremia carp virus (SVCV) suggest preventive drug candidates. PLoS One 8, e73553.

Encinas, P., Rodriguez-Milla, M.A., Novoa, B., Estepa, A., Figueras, A., Coll, J.M., 2010. Zebrafish fin immune responses during high mortality infections with viral haemorrhagic septicemia rhabdovirus. A proteomic and transcriptomic approach. BMC Genomics 11, 518–534.

Enocsson, H., Sjowall, C., Skogh, T., Eloranta, M.L., Ronnblom, L., Wettero, J., 2009. Interferon-alpha mediates suppression of C-reactive protein: explanation for muted C-reactive protein response in lupus flares? Arthritis Rheum 60, 3755–3760.

Estepa, A., Coll, J., 2015a. Innate Multigene Family Memories Are Implicated in the Viral-Survivor Zebrafish Phenotype. PLoS One 10, e0135483.

Estepa, A., Coll, J.M., 1996. Pepscan mapping and fusion related properties of the major phosphatidylserine-binding domain of the glycoprotein of viral hemorrhagic septicemia virus, a salmonid rhabdovirus. Virology 216, 60–70.

Estepa, A., Coll, J.M., 2015b. Innate multigene family memories are implicated in the viral-survivor zebrafish phenotype. Plos One 10, e0135483.

Estepa, A.M., Rocha, A.I., Mas, V., Perez, L., Encinar, J.A., Nunez, E., Fernandez, A., Ros, J.M.G., Gavilanes, F., Coll, J.M., 2001. A protein G fragment from the Salmonid viral hemorrhagic septicemia rhabdovirus induces cell-to-cell fusion and membrane phosphatidylserine translocation at low pH. Journal of Biological Chemistry 276, 46268–46275.

Falco, A., Cartwright, J.R., Wiegertjes, G.F., Hoole, D., 2012. Molecular characterization and expression analysis of two new C-reactive protein genes from common carp (Cyprinus carpio). Dev Comp Immunol 37, 127–138.

Falco, A., Chico, V., Marroqui, L., Perez, L., Coll, J.M., Estepa, A., 2008. Expression and antiviral activity of a beta-defensin-like peptide identified in the rainbow trout (Oncorhynchus mykiss) EST sequences. Mol Immunol 45, 757–765.

Fijan, N., Petrinec, Z., Sulimanovic, D., Zwillenberg, L.O., 1971. Isolation of the viral causative agent from the acute form of infectious dropsy of carp. Veterinary Archives 41, 125–138.

Garcia-Valtanen, P., Martinez-Lopez, A., Lopez-Munoz, A., Bello-Perez, M., Medina-Gali, R.M., Ortega-Villaizan, M.D., Varela, M., Figueras, A., Mulero, V., Novoa, B., Estepa, A., Coll, J., 2017. Zebra Fish Lacking Adaptive Immunity Acquire an Antiviral Alert State Characterized by Upregulated Gene Expression of Apoptosis, Multigene Families, and Interferon-Related Genes. Front Immunol 8, 121.

Genge, C.E., Lin, E., Lee, L., Sheng, X., Rayani, K., Gunawan, M., Stevens, C.M., Li, A.Y., Talab, S.S., Claydon, T.W., Hove-Madsen, L., Tibbits, G.F., 2016. The Zebrafish Heart as a Model of Mammalian Cardiac Function. Rev Physiol Biochem Pharmacol 171, 99–136.

Harmache, A., Leberre, M., Droineau, S., Giovannini, M., Bremont, M., 2006. Bioluminescence Imaging of Live Infected Salmonids Reveals that the Fin Bases Are the Major Portal of Entry for Novirhabdovirus. Journal Virology 103, 3655–3659.

Huang, W.C., Hsieh, Y.S., Chen, I.H., Wang, C.H., Chang, H.W., Yang, C.C., Ku, T.H., Yeh,

S.R., Chuang, Y.J., 2010. Combined use of MS-222 (tricaine) and isoflurane extends anesthesia time and minimizes cardiac rhythm side effects in adult zebrafish. Zebrafish 7, 297–304.

ICTV, 2015. Implementation of taxon-wide non-Latinized binomial species names in the family Rhabdoviridae Rhabdoviridae Study Group, 9.

Ishihama, Y., Oda, Y., Tabata, T., Sato, T., Nagasu, T., Rappsilber, J., Mann, M., 2005. Exponentially modified protein abundance index (emPAI) for estimation of absolute protein amount in proteomics by the number of sequenced peptides per protein. Mol Cell Proteomics 4, 1265–1272.

Kindmark, C.O., 1971. Stimulating effect of C-reactive protein on phagocytosis of various species of pathogenic bacteria. Clin Exp Immunol 8, 941–948.

LeBerre, M., De Kinkelin, P., Metzger, A., 1977. Identification sérologique des rhabdo-virus des salmonidés. Bulletin Office International Epizooties 87, 391–393.

Li, H.Y., Wang, J., Meng, F., Jia, Z.K., Su, Y., Bai, Q.F., Lv, L.L., Ma, F.R., Potempa, L.A., Yan, Y.B., Ji, S.R., Wu, Y., 2016. An Intrinsically Disordered Motif Mediates Diverse Actions of Monomeric C-reactive Protein. J Biol Chem 291, 8795–8804.

Livak, K.L., Schmittgen, T.D., 2001. Analysis of Relative Gene Expression Data Using Real-Time Quantitative PCR and the 2 –DDCT Method. Methods 25, 402–408.

Lopez-Munoz, A., Roca, F.J., Sepulcre, M.P., Meseguer, J., Mulero, V., 2010. Zebrafish larvae are unable to mount a protective antiviral response against waterborne infection by spring viremia of carp virus. Developmental Comparative Immunology 34, 546–552.

Lu, F., Langenbacher, A.D., Chen, J.N., 2016. Transcriptional Regulation of Heart Development in Zebrafish. J Cardiovasc Dev Dis 3.

Lu, J., Marjon, K.D., Mold, C., Du Clos, T.W., Sun, P.D., 2012. Pentraxins and Fc receptors. Immunol Rev 250, 230–238.

Mantel, N., 1966. Evaluation of survival data and two new rank order statistics arising in its consideration. Cancer Chemother Rep 50, 163–170.

McKibben, R.A., Haberlen, S.A., Post, W.S., Brown, T.T., Budoff, M., Witt, M.D., Kingsley, L.A., Palella Jr., F.J., Thio, C.L., Seaberg, E.C., 2016. A Cross-sectional Study of the Association Between Chronic Hepatitis C Virus Infection and Subclinical Coronary Atherosclerosis Among Participants in the Multicenter AIDS Cohort Study. J Infect Dis 213, 257–265.

Novoa, B., Romero, A., Mulero, V., Rodriguez, I., Fernandez, I., Figueras, A., 2006. Zebrafish (Danio rerio) as a model for the study of vaccination against viral hae-morrhagic septicemia virus (VHSV). Vaccine 24, 5806–5816.

Paludan, S.R., 2001. Requirements for the induction of interleukin-6 by herpes simplex virus-infected leukocytes. J Virol 75, 8008–8015.

Pereiro, P., Forn-Cuni, G., Dios, S., Coll, J., Figueras, A., Novoa, B., 2017. Interferon-independent antiviral activity of 25-hydroxycholesterol in a teleost fish. Antiviral Res 145, 146–159.

Pionnier, N., Adamek, M., Miest, J.J., Harris, S.J., Matras, M., Rakus, K.L., Irnazarow, I., Hoole, D., 2014. C-reactive protein and complement as acute phase reactants in common carp Cyprinus carpio during CyHV-3 infection. Dis Aquat Organ 109, 187–199.

Pitto, L., Chiavacci, E., Burchielli, S., Dolfi, L., Zozzini, E.T., Priami, C., Cellerino, A., Cremisi, F., 2011. Zebrafish as Model System for Studying the Transcription Factor/miRNA Regulative Network in Brain and Heart Development. Journal of the American Association for Laboratory Animal Science 50 743–743.

Potempa, L.A., Yao, Z.Y., Ji, S.R., Filep, J.G., Wu, Y., 2015. Solubilization and purification of recombinant modified C-reactive protein from inclusion bodies using reversible anhydride modification. Biophys Rep 1, 18–33.

Rocha, A., Ruiz, S., Coll, J.M., 2005. Improvement of transfection efficiency of epithe-lioma papulosum cyprini carp cells by modification of their cell cycle and using an optimal promoter. Marine Biotechnology 6, 401–410.

Sanders, G.E., Batts, W.N., Winton, J.R., 2003. Susceptibility of zebrafish (Danio rerio) to a model pathogen, spring viremia of carp virus. Comp Med 53, 514–521.

Shah, S., Ma, Y., Scherzer, R., Huhn, G., French, A.L., Plankey, M., Peters, M.G., Grunfeld, C., Tien, P.C., 2015. Association of HIV, hepatitis C virus and liver fibrosis severity with interleukin-6 and C-reactive protein levels. AIDS 29, 1325–1333.

Shephard, E.G., Beer, S.M., Anderson, R., Strachan, A.F., Nel, A.E., de Beer, F.C., 1989. Generation of biologically active C-reactive protein peptides by a neutral protease on the membrane of phorbol myristate acetate-stimulated neutrophils. J Immunol 143, 2974–2981.

Shrivastava, A.K., Singh, H.V., Raizada, A., Singh, S.K., 2015. C-reactive protein, in-flammation and coronary heart disease. The Egyptian Heart Journal 67, 89–97.

Sunyer, J.O., 2013. Fishing for mammalian paradigms in the teleost immune system. Nat Immunol 14, 320–326.

Sunyer, J.O., Zarkadis, I.K., Lambris, J.D., 1998. Complement diversity: a mechanism for generating immune diversity? Immunol Today 19, 519–523.

Varela, M., Figueras, A., Novoa, B., 2016. Modelling viral infections using zebrafish: Innate immune response and antiviral research. Antiviral Res 139, 59–68.

Varela, M., Romero, A., Dios, S., van der Vaart, M., Figueras, A., Meijer, A.H., Novoa, B., 2014. Cellular visualization of macrophage pyroptosis and interleukin-1beta release in a viral hemorrhagic infection in zebrafish larvae. J Virol 88, 12026–12040.

Vilahur, G., Badimon, L., 2015. Biological actions of pentraxins. Vascul Pharmacol 73, 38–44.

Voulgaris, T., Sevastianos, V.A., 2016. Atherosclerosis as Extrahepatic Manifestation of Chronic Infection with Hepatitis C Virus. Hepat Res Treat 2016, 7629318.

Wang, J., Wang, Q., Han, T., Li, Y.K., Zhu, S.L., Ao, F., Feng, J., Jing, M.Z., Wang, L., Ye, L.B., Zhu, Y., 2015. Soluble interleukin-6 receptor is elevated during influenza A virus infection and mediates the IL-6 and IL-32 inflammatory cytokine burst. Cell Mol Immunol 12, 633–644.

Wang, M.Y., Ji, S.R., Bai, C.J., El Kebir, D., Li, H.Y., Shi, J.M., Zhu, W., Costantino, S., Zhou, H.H., Potempa, L.A., Zhao, J., Filep, J.G., Wu, Y., 2011. A redox switch in C-reactive protein modulates activation of endothelial cells. FASEB J 25, 3186–3196.

Wu, Y., Potempa, L.A., El Kebir, D., Filep, J.G., 2015. C-reactive protein and inflamma-tion: conformational changes affect function. Biol Chem 396, 1181–1197.

Wu, Y.P., Sun, D.D., Wang, Y., Liu, W., Yang, J., 2016. Herpes Simplex Virus Type 1 and Type 2 Infection Increases Atherosclerosis Risk: Evidence Based on a Meta-Analysis. Biomed Res Int 2016, 2630865.

Xia, C., Liu, Y., Chen, Z., Zheng, M., 2015. Involvement of Interleukin 6 in Hepatitis B Viral Infection. Cell Physiol Biochem 37, 677–686.

Yavin, E.J., Fridkin, M., 1998. Peptides derived from human C-reactive protein inhibit the enzymatic activities of human leukocyte elastase and cathepsin G: use of overlapping peptide sequences to identify a unique inhibitor. J Pept Res 51, 282–289.

Zhang, Y.A., Salinas, I., Li, J., Parra, D., Bjork, S., Xu, Z., LaPatra, S.E., Bartholomew, J., Sunyer, J.O., 2010. IgT, a primitive immunoglobulin class specialized in mucosal immunity. Nat Immunol 11, 827–835.